



**HAL**  
open science

## Tube/projectile interaction modeling using finite element simulation

Thomas Collas, Frédéric Lebon, Iulian Rosu, Corado Ningre

### ► To cite this version:

Thomas Collas, Frédéric Lebon, Iulian Rosu, Corado Ningre. Tube/projectile interaction modeling using finite element simulation. ICCCM 2023 - VII International Conference on Computational Contact Mechanics, Jul 2023, Torino, Italy. hal-04186917

**HAL Id: hal-04186917**

**<https://hal.science/hal-04186917v1>**

Submitted on 12 Apr 2024

**HAL** is a multi-disciplinary open access archive for the deposit and dissemination of scientific research documents, whether they are published or not. The documents may come from teaching and research institutions in France or abroad, or from public or private research centers.

L'archive ouverte pluridisciplinaire **HAL**, est destinée au dépôt et à la diffusion de documents scientifiques de niveau recherche, publiés ou non, émanant des établissements d'enseignement et de recherche français ou étrangers, des laboratoires publics ou privés.



Laboratoire de Mécanique et d'Acoustique

**KNDS**

# Tube/projectile interaction modeling using finite element method

---

T. COLLAS, F. LEBON, I. ROSU and C. NINGRE.

7th International Conference on Computational Contact Mechanics, July 5-7, 2023, Torino - Italy



## Introduction

### I. Analytical model

- a) Rigid cone
- b) Elastic cone

### II. Finite element models

- a) Quasi-statics
- b) Dynamics

## Conclusion

- Manage the loading/unloading cycle of the artillery projectile:

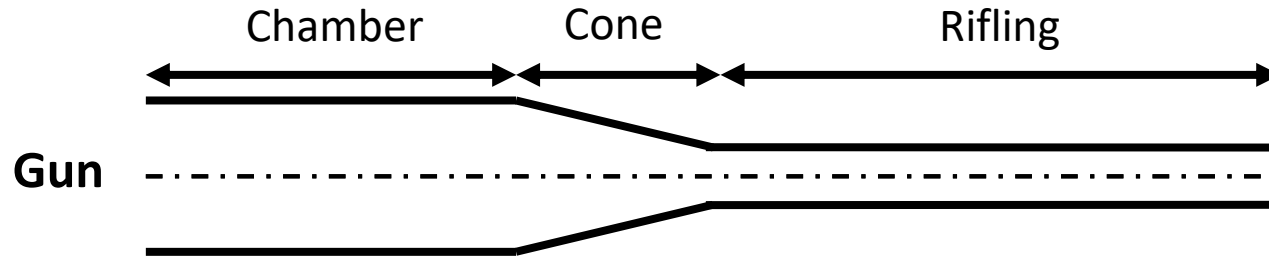


Fig. 1. Gun barrel.



Fig. 2. Projectile.

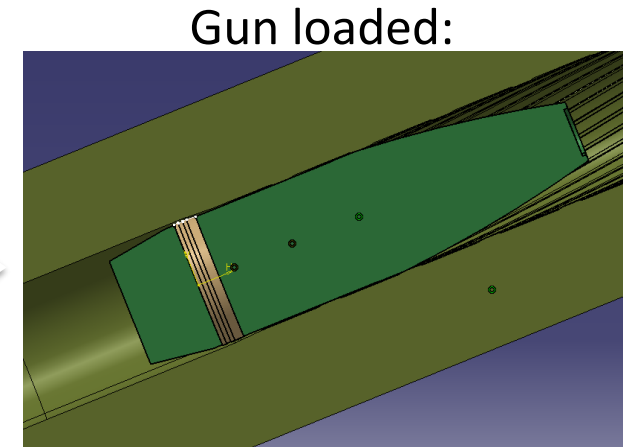
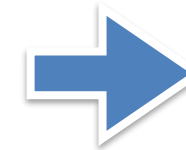


Fig. 3. Loaded projectile.

➔ Conical shrink fit assembly

- Objective: Focus on shrink fit assembly

- Non-linearities to take into account:

Elastic-plastic material

Complex geometries

Contact + Friction

Finite strain ( $\approx 30\%$  locally)

# I.a) Analytical model – Rigid cone

- Cone to cone interaction with no strain:

Principles of statics:

- $E_p = PS \left( \frac{\mu_p}{\tan(\alpha/2)} + 1 \right)$
- $E_{ex} = -PS \left( \frac{\mu_{ex}}{\tan(\alpha/2)} - 1 \right)$

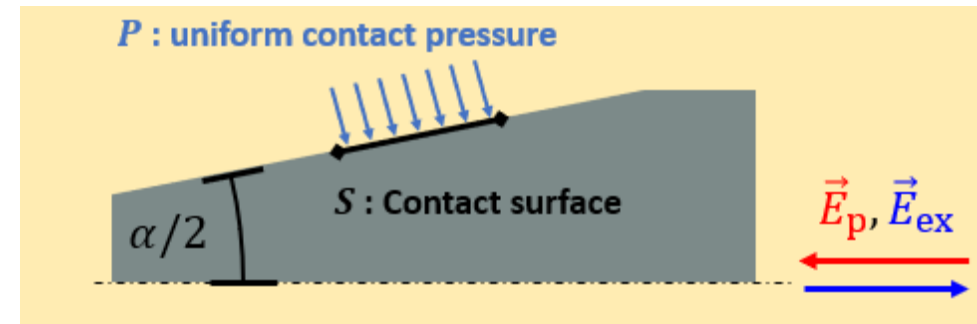


Fig. 4. Rigid cone model.

- “Reaction” factor:

$$r_{\text{rigid}} = \frac{-E_{ex}}{E_p} = \frac{\mu_{ex} - \tan(\alpha/2)}{\mu_p + \tan(\alpha/2)}$$

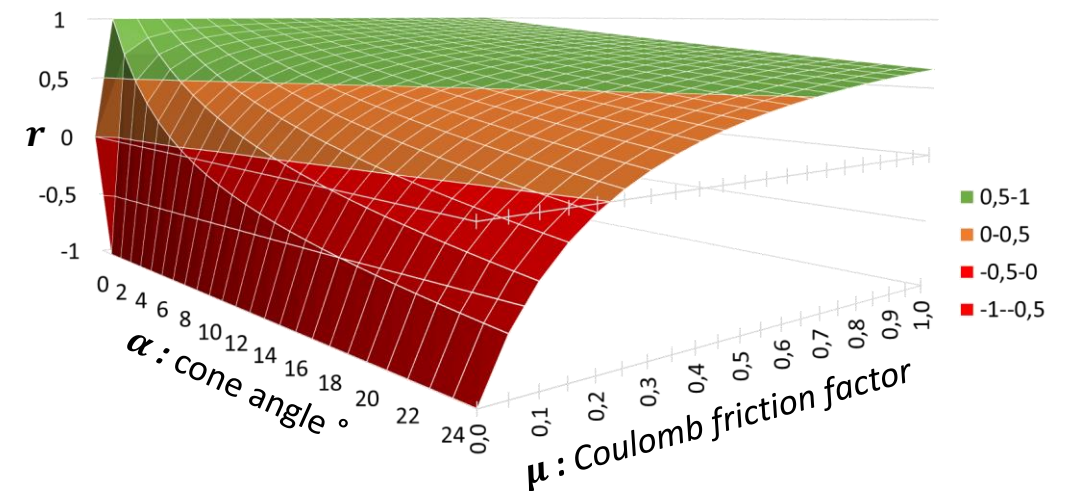


Fig. 5. r response.

- Extraction force is lower than penetration force.

# I.b) Analytical model – Elastic cone

➤ Adding an elastic behaviour:

- Obtaining a 3 steps model:

1. **p**enetration: push into cone ;
2. **s**pringback: partial relief of stress ;
3. **e**xtraction: pull until contact loss.

- 1.  $\rightarrow \frac{F_{x,p}}{F_{y,p}} = \frac{1 - \mu_p \tan(\alpha/2)}{\mu_p + \tan(\alpha/2)}$  et 3.  $\rightarrow \frac{F_{x,ex}}{F_{y,ex}} = \frac{1 + \mu_{ex} \tan(\alpha/2)}{-\mu_{ex} + \tan(\alpha/2)}$

- Leads to:  $r_{elastic} = \frac{-E_{ex}}{E_p} = r_{rigid} \frac{1 - \mu_p \tan(\alpha/2)}{1 + \mu_{ex} \tan(\alpha/2)}$

➤ « Inversion » factor :

$$f_{inv} = \frac{1 - \mu_p \tan(\alpha/2)}{1 + \mu_{ex} \tan(\alpha/2)}$$

➤ New factor describing the evolution of loading direction.

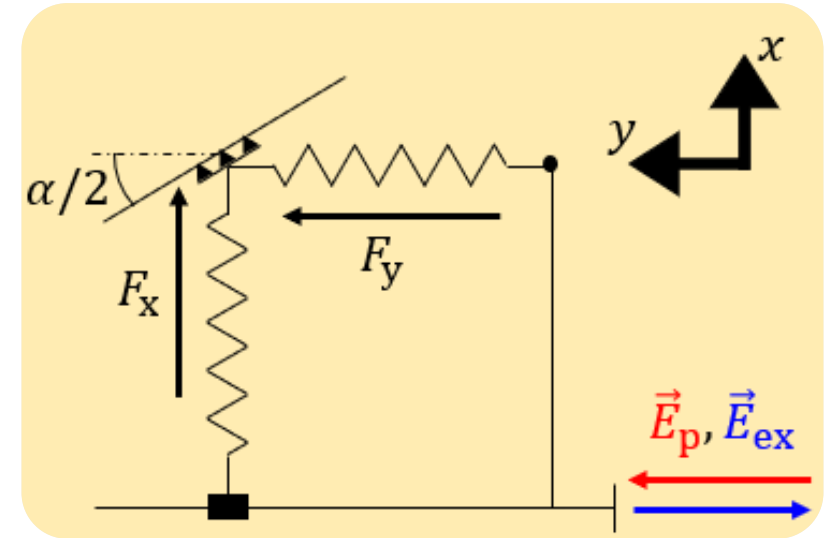


Fig. 6. Elastic cone model.

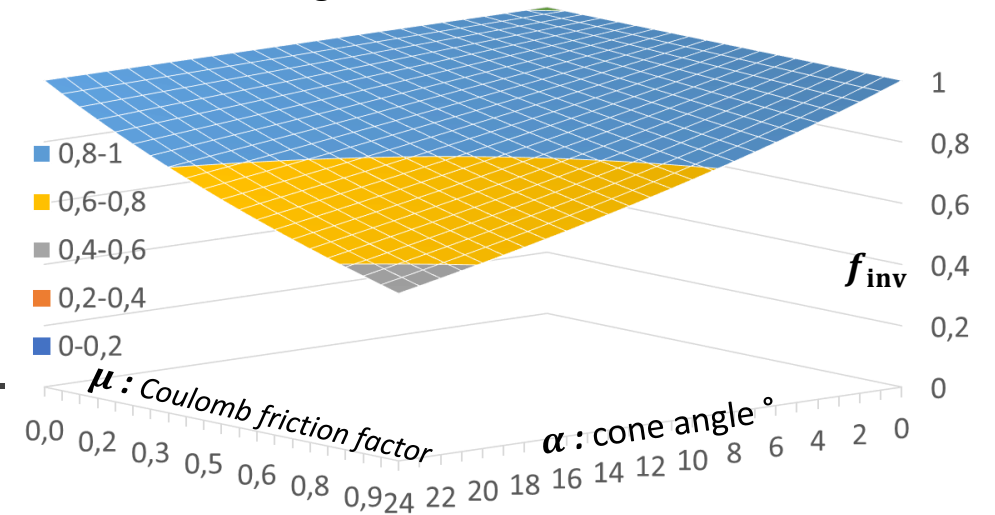


Fig. 7.  $f_{inv}$  response surface.

## II.a) Finite element models – Quasi-statics

➤ Axisymmetric numerical model:

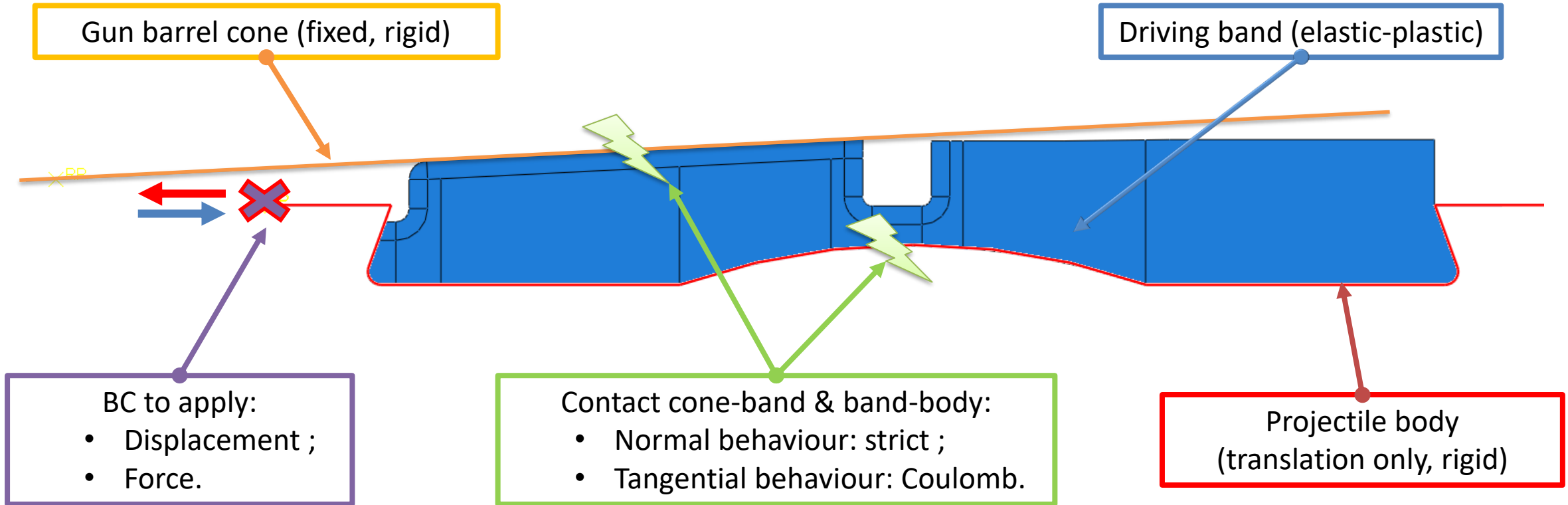


Fig. 8. Quasi-static model formulation.

■ Simulation in three steps :

1) Penetration

2) Springback

3) Extraction

## II.a) Finite element models – Quasi-statics

- von Mises stress during the three steps:

Step: Penetrat Frame: 0  
 Total Time: 0.000000

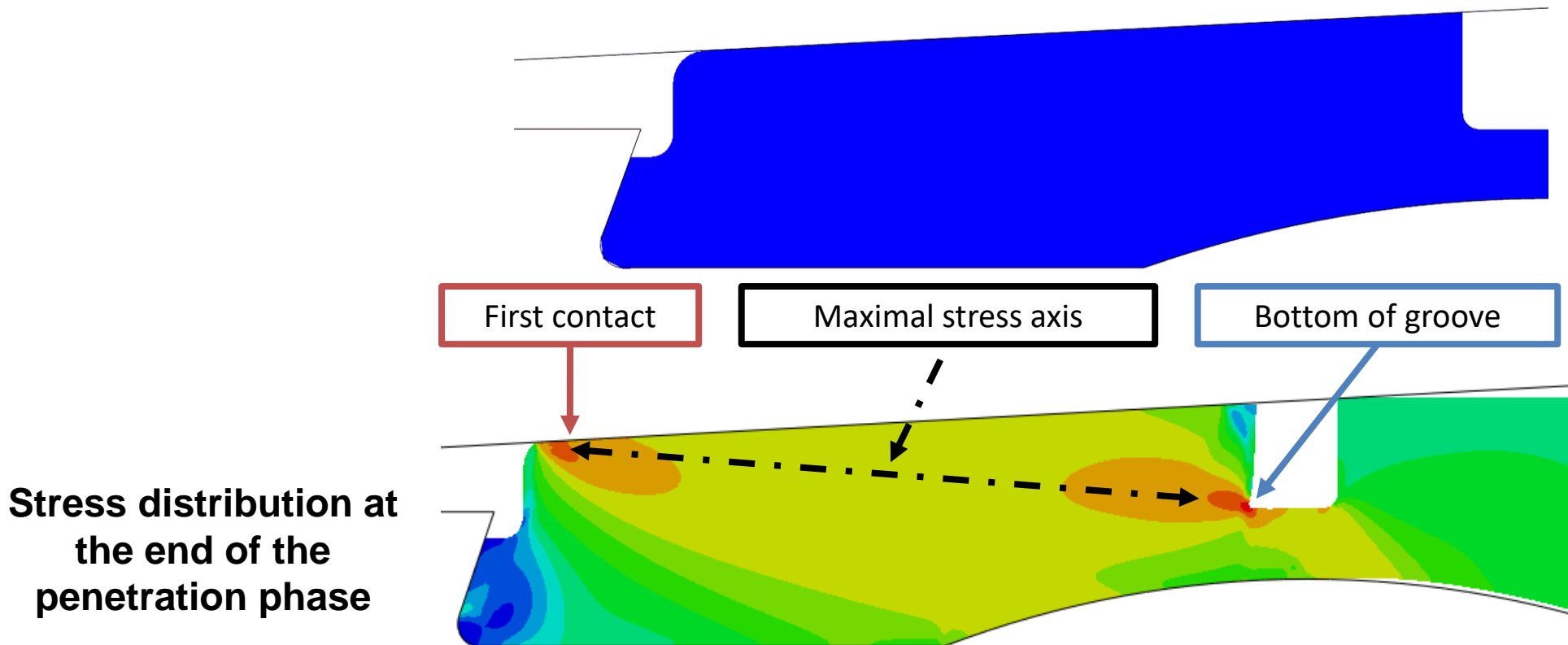


Fig. 11. von Mises stress color map.

- Typical stress repartition due to geometry. I obtain:  $r_{\text{simulated}} = \frac{-E_{\text{ex}}}{E_{\text{p}}}$



➤ Mesh optimisation on extraction force:

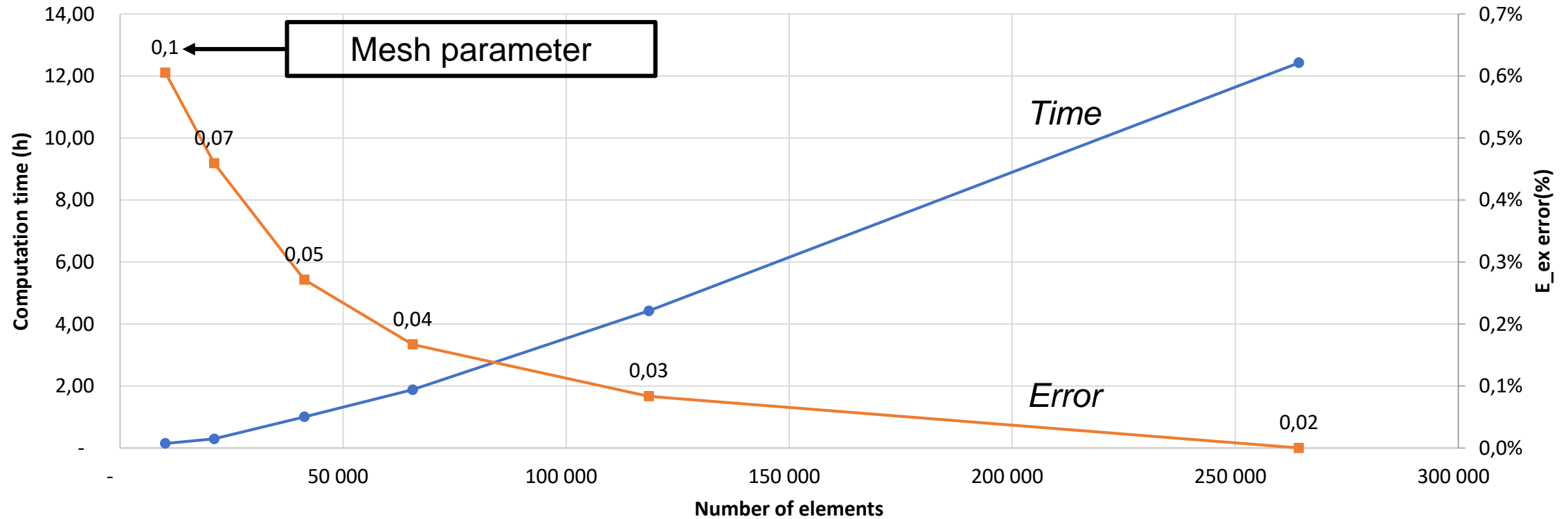


Fig. 12. Performances of an homogeneously meshed band.

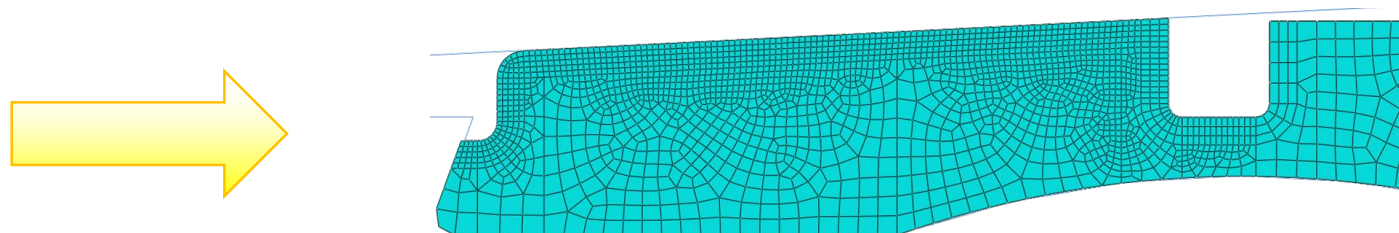


Fig. 13. Axisymmetric adapted mesh (2868 elements).

## II.a) Finite element models – Quasi-statics

➤ Pressure – Overclosure ( $P - o$ ) relationships for normal contact:

- Strict : “hard contact”

- $\forall P, o \leq 0$  ;

- Linear :

- $P = K_0 * o$  ;

- Exponential :

- $P = \frac{P_0}{\exp(1)-1} \left( \frac{o}{C_0} + 1 \right) \left( \exp\left( \frac{o}{C_0} + 1 \right) - 1 \right)$ .

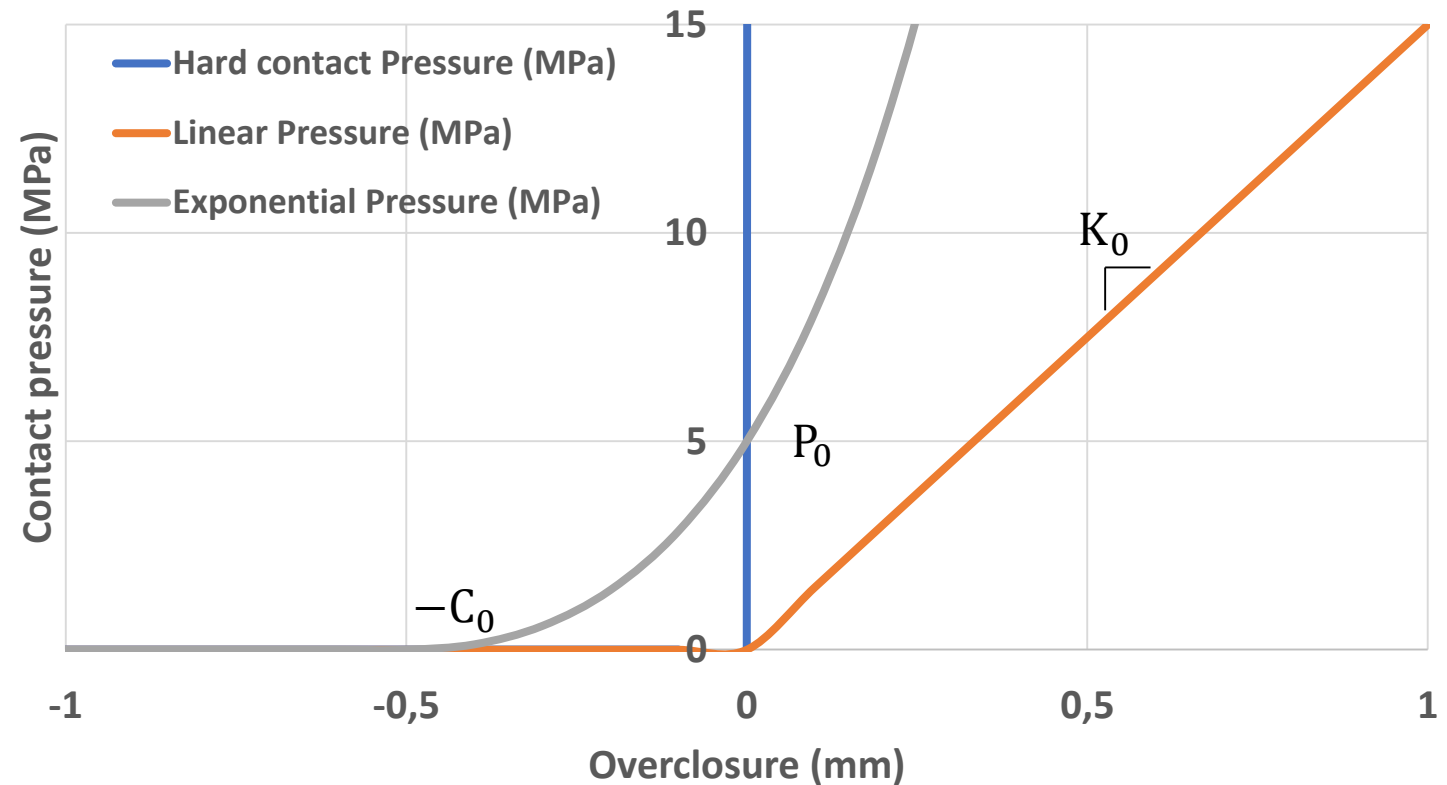


Fig. 14. Normal contact laws.

## II.a) Finite element models – Quasi-statics

➤ Comparison of soft and hard contact laws:

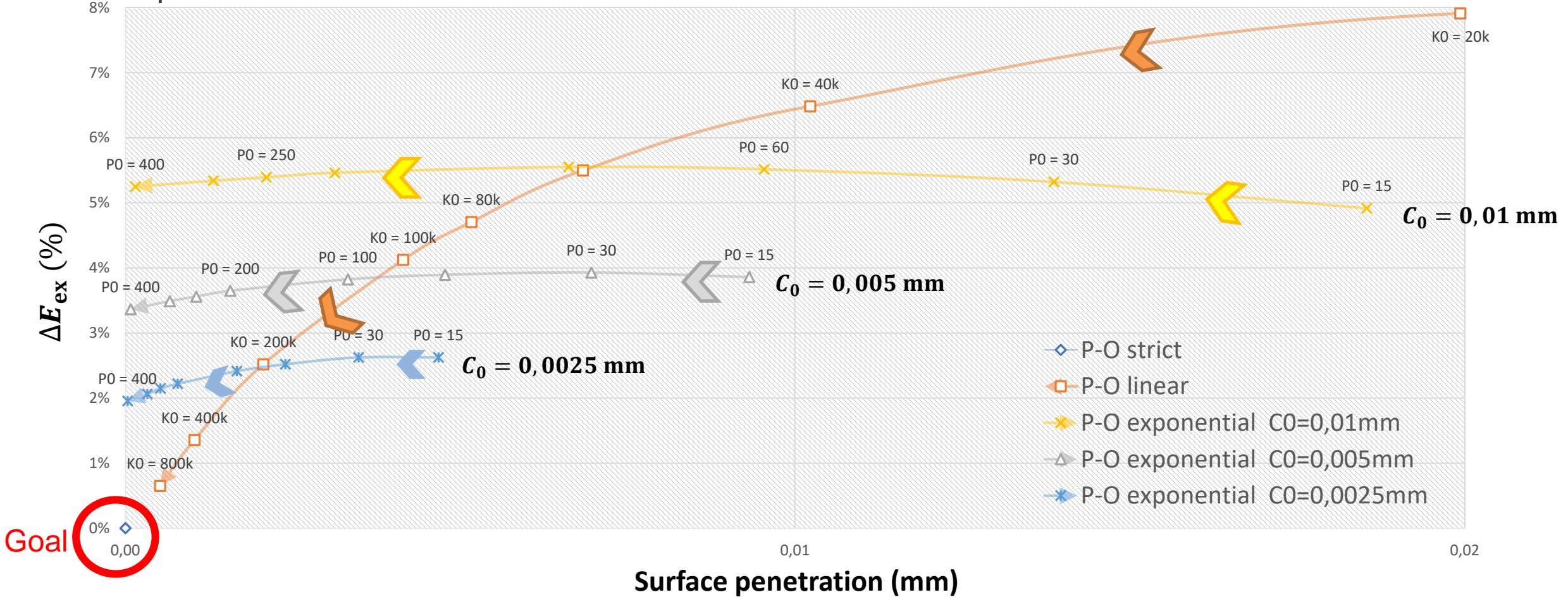
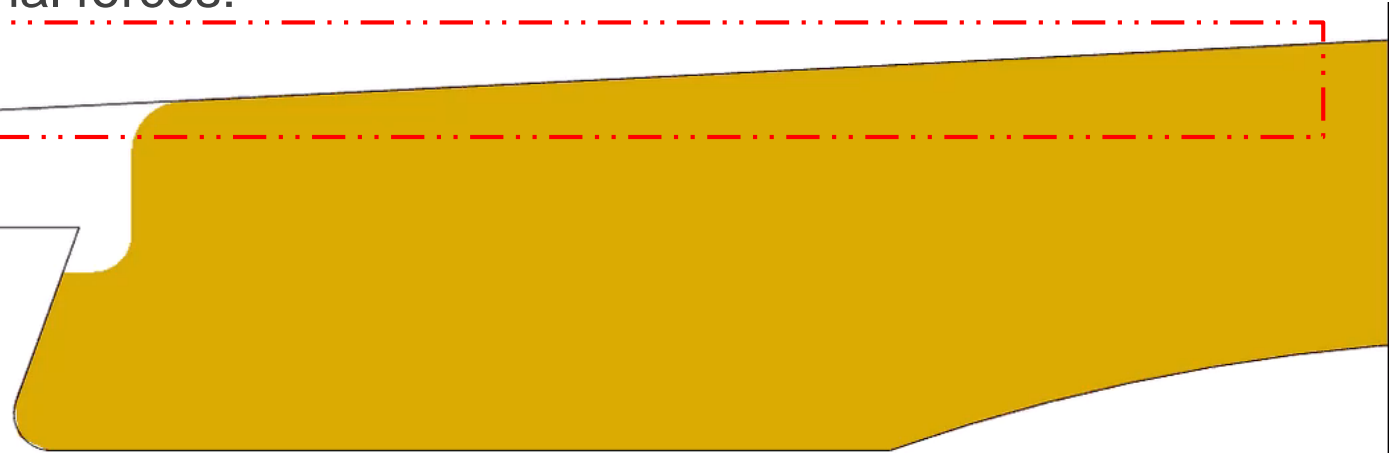


Fig. 15. Comparison of normal contact strategies accuracies.

➤ Bias can be reduced by “hardening” the law.

➤ Plotting the external forces:

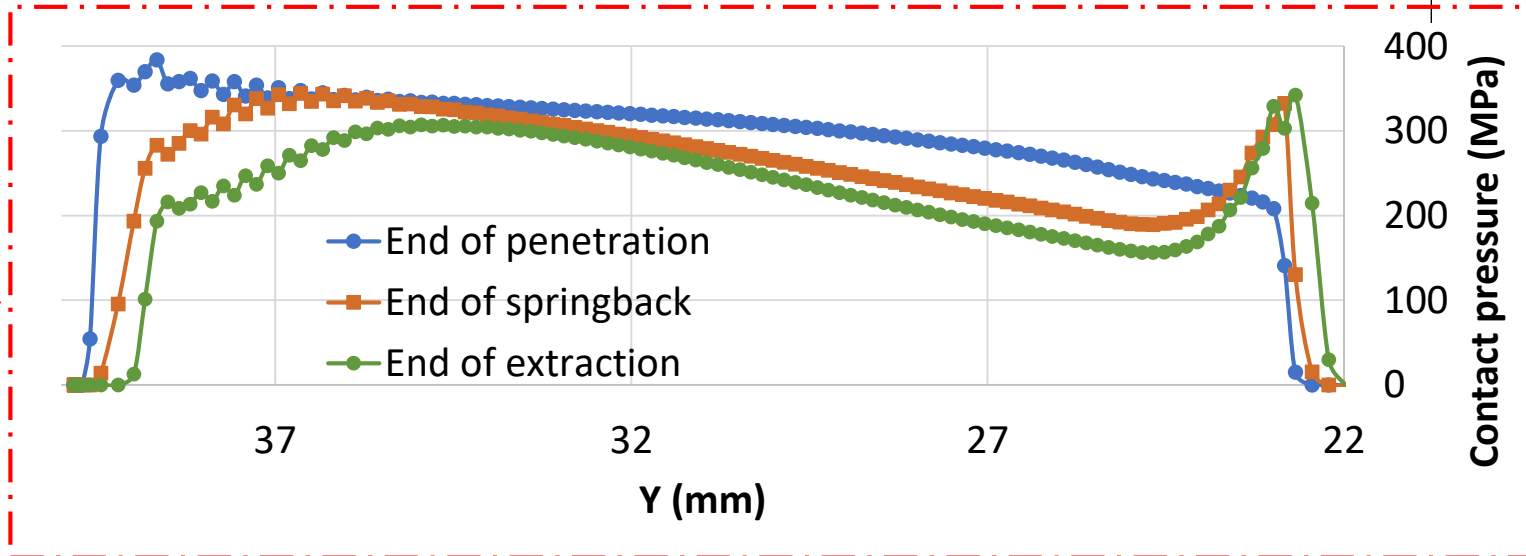
Fig. 16. Nodal force evolution.



Step: Penetrat Frame: 0  
 Total Time: 0.000000

At the end of each step, we plot the pressure distribution.

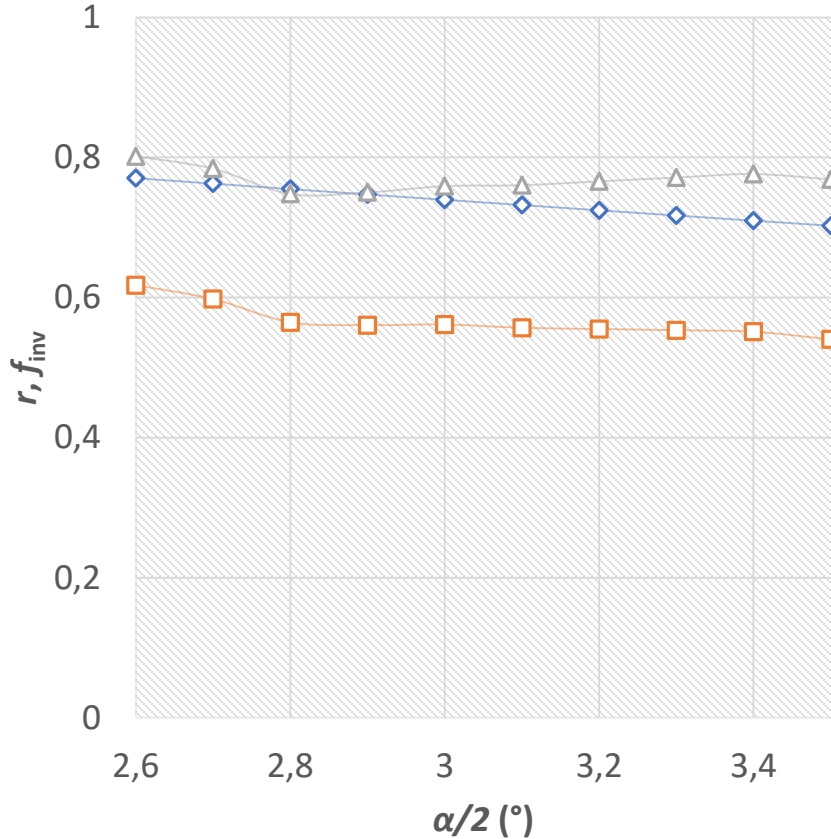
Fig. 17. Pressure evolution at the interface.



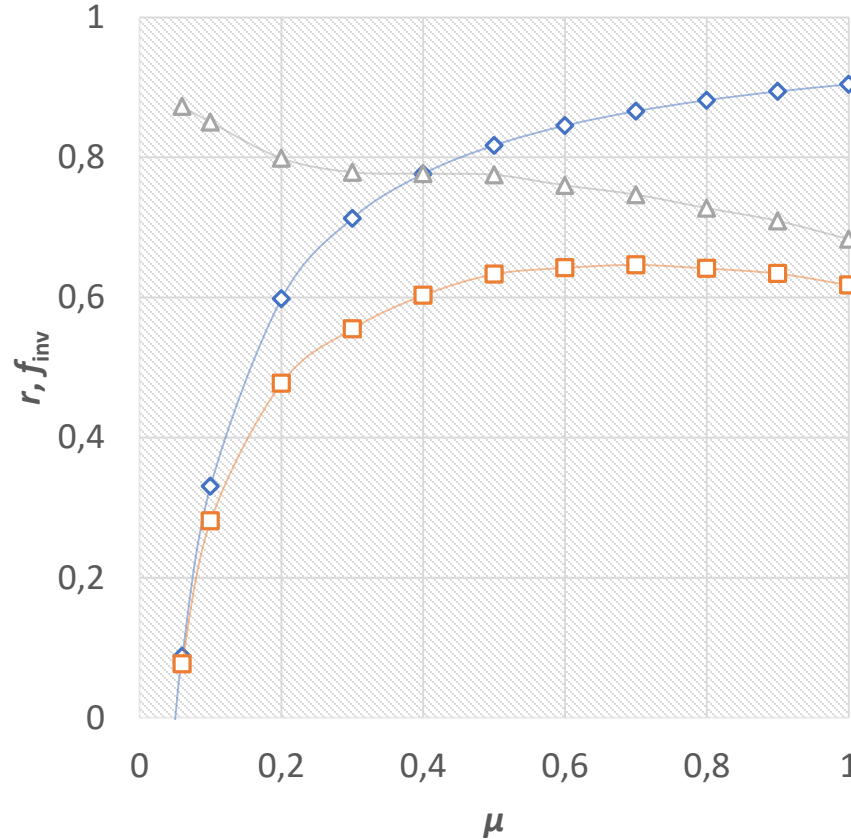
➤ Heterogeneous contact pressure evolving with loading.

## II.a) Finite element models – Quasi-statics

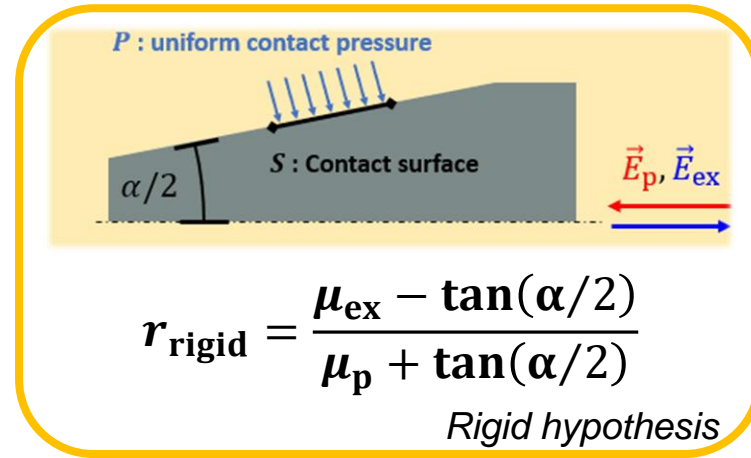
➤ Input parameters sensitivity:



—◇—  $r_{rigid}$  —□—  $r_{simulated}$  —△—  $f_{inv}$



—◇—  $r_{rigid}$  —□—  $r_{simulated}$  —△—  $f_{inv}$



$$r_{simulated} = \frac{-E_{ex}}{E_p}$$

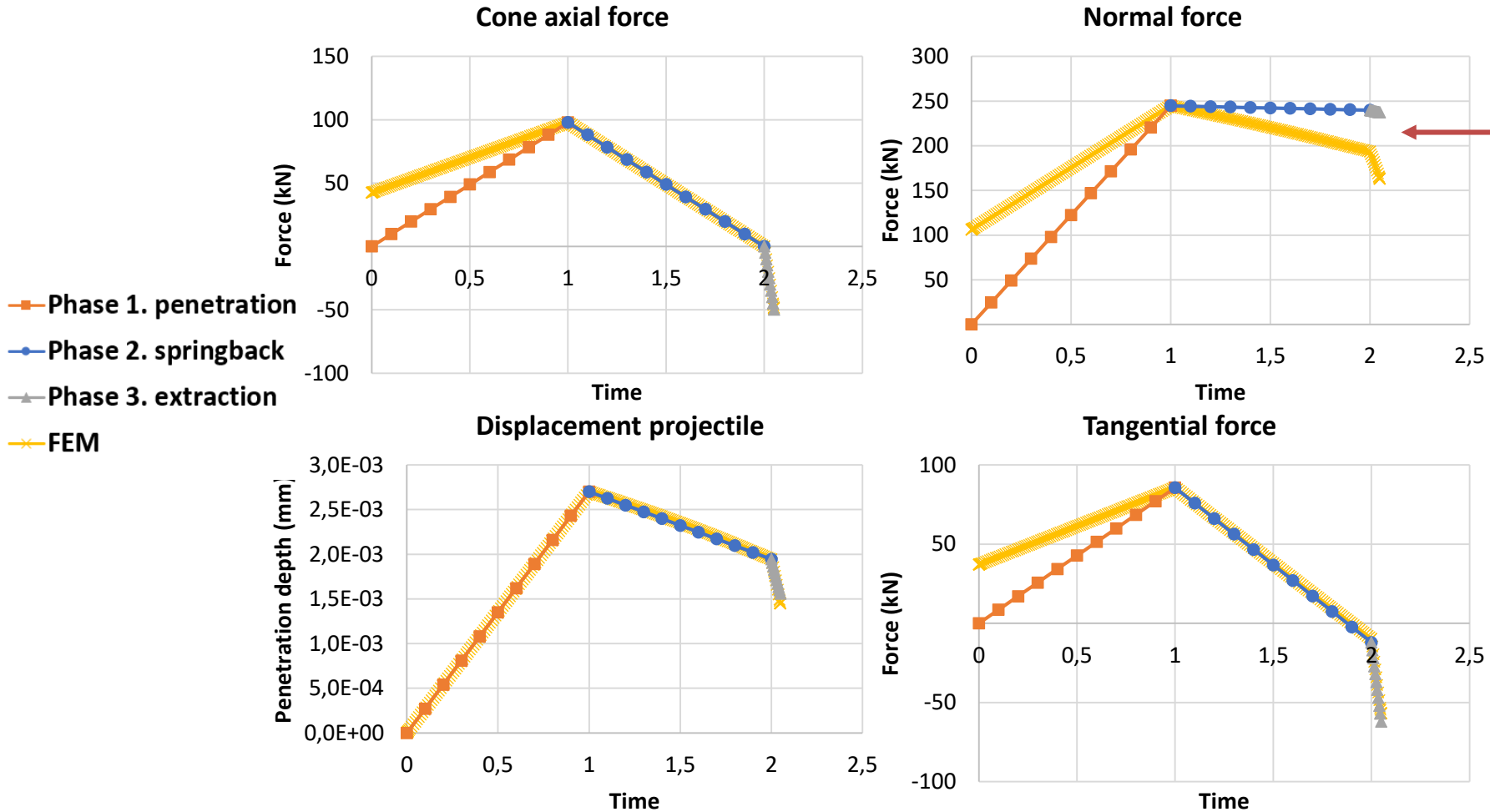
$$f_{inv} = \frac{r_{simulated}}{r_{rigid}}$$

Fig. 18. Influence of cone angle  $\alpha$  and friction coefficient  $\mu$  on  $r$  and  $f_{inv}$ .

➤ For typical cone angles,  $\mu$  is more impactful than  $\alpha$ .

## II.a) Finite element models – Quasi-statics

- Comparison between FEM and analytical model. Temporals of the elastic model:



Discrepancies in the evolution of normal force.

Analytical/FEM error	
Position	Force
0,05%-0,6%	20%-40%

Fig. 19. Comparison between FEM and elastic model for interface variables.

- Elastic model qualitatively describes the phenomena.

➤ Axisymmetric numerical model:

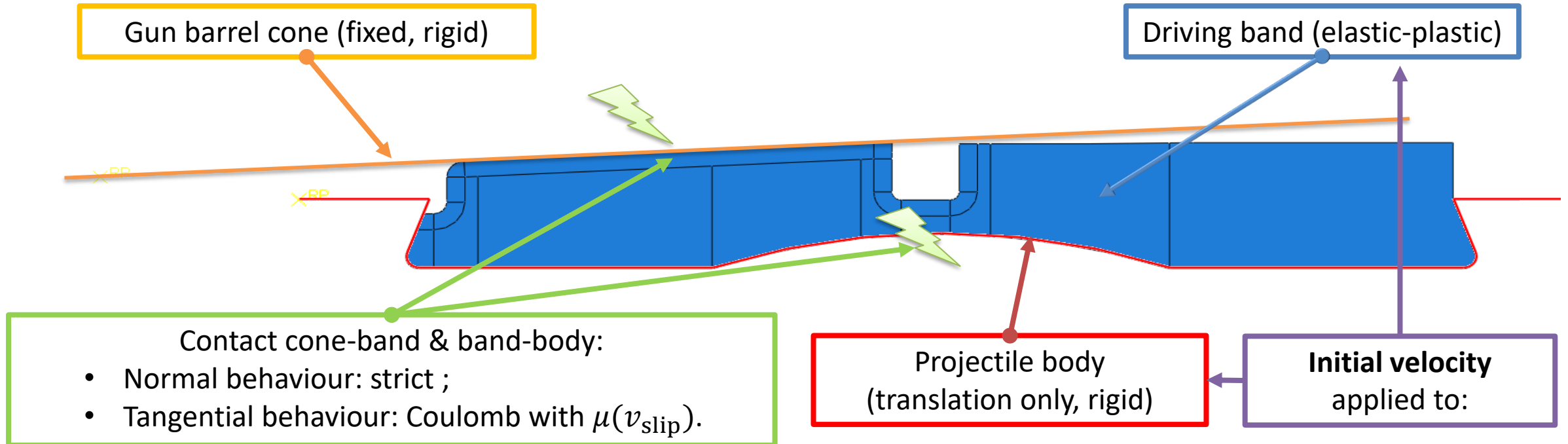


Fig. 20. Dynamic model formulation.

- Simulation in two steps :
  - 1) & 2) Penetration & springback
- Using same mesh than quasi-statics.

c) Extraction

➤ Dynamic implicit results for  $v_{ini} = 1 \text{ m.s}^{-1}$  :

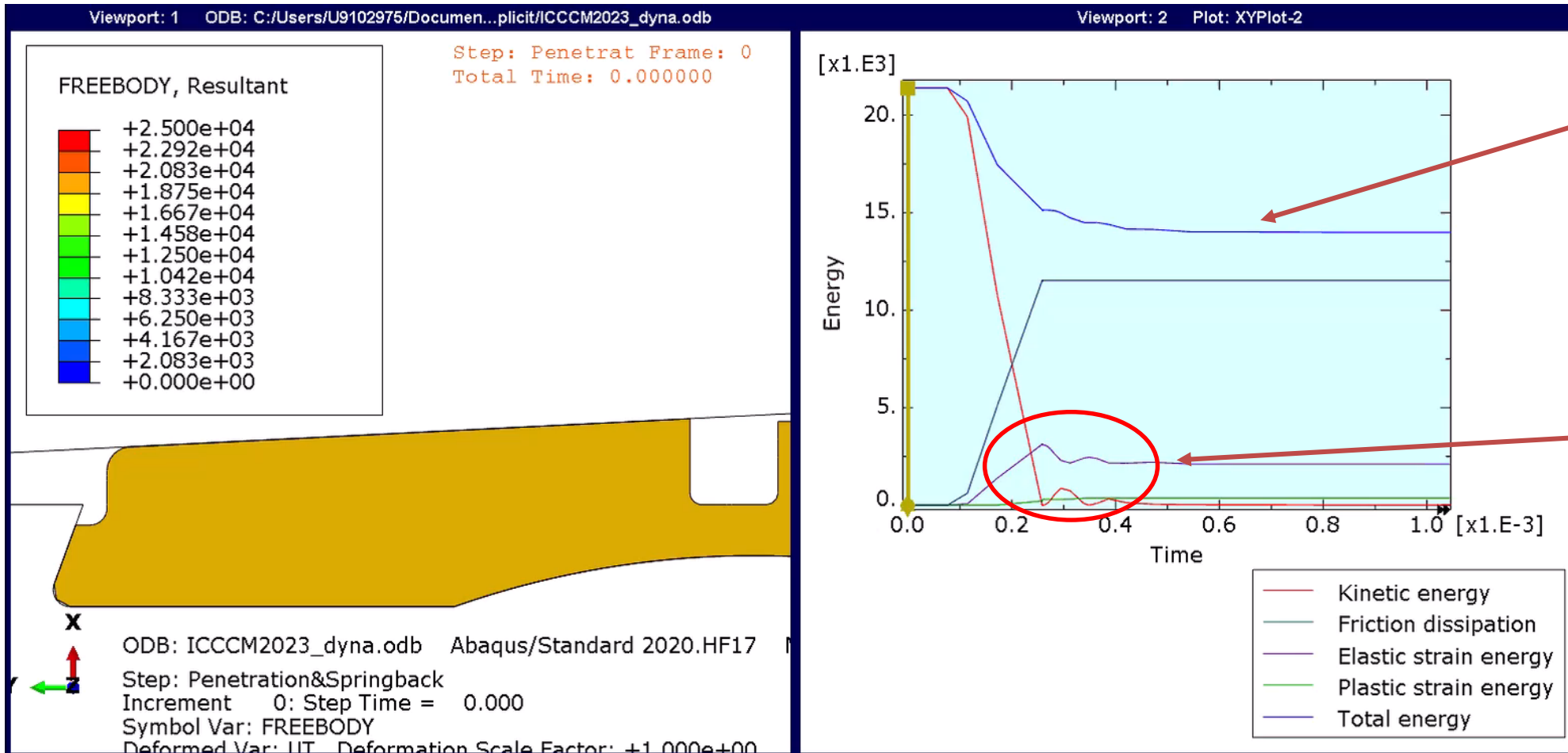


Fig. 21. Nodal forces evolution.

Fig. 22. Energies evolution.

➤ The elastic wave is quite costly in terms of computation time.



- Extraction force comparison for static and dynamic implicit simulations:

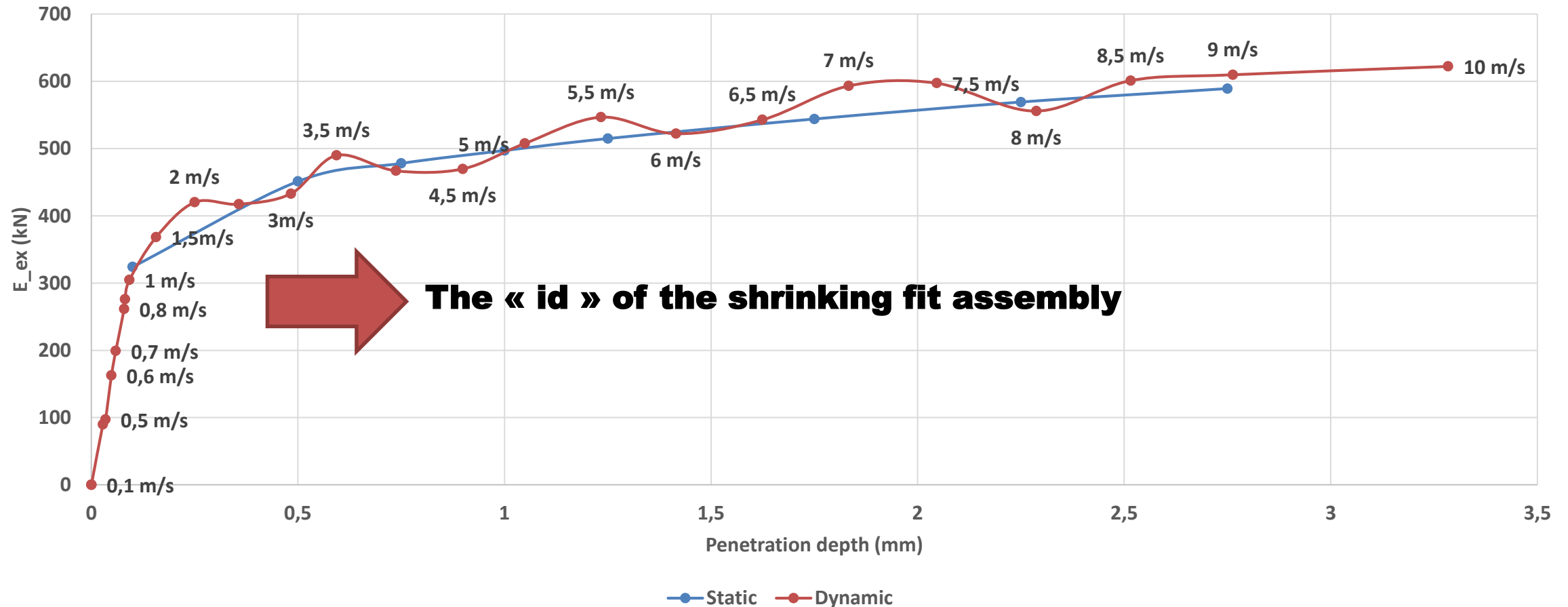


Fig. 23.  $E_{ex}$  (penetration depth) for quasi-statics and dynamics implicit models.

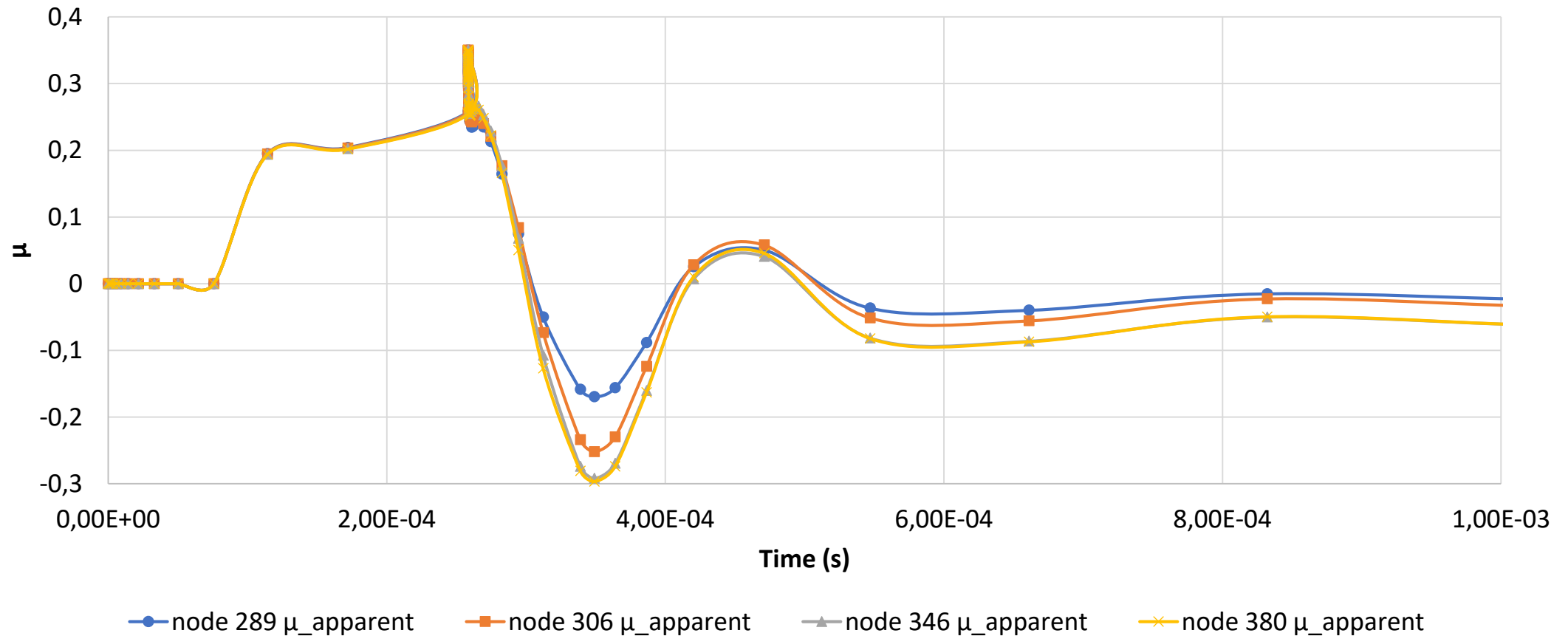
- Good tendency adequation but oscillations have to be managed.

- FEM as a tool for research in difficult access area.
- No large discrepancy between analytical or FEM model identified ;
- Theoretical demonstration of  $-E_{ex} < E_p$  ;
- $\mu$  is the most important parameter in a conical shrink fit assembly ;
- Further developments:
  - Experimental campaign to validate the numerical results ;
  - Analytical model have to be enhanced.

**THANK YOU FOR LISTENING !**

**Now it is time for questions !**

- Looking at some nodes at the interface (dynamic implicit simulation):



➤ Main simulation parameters:

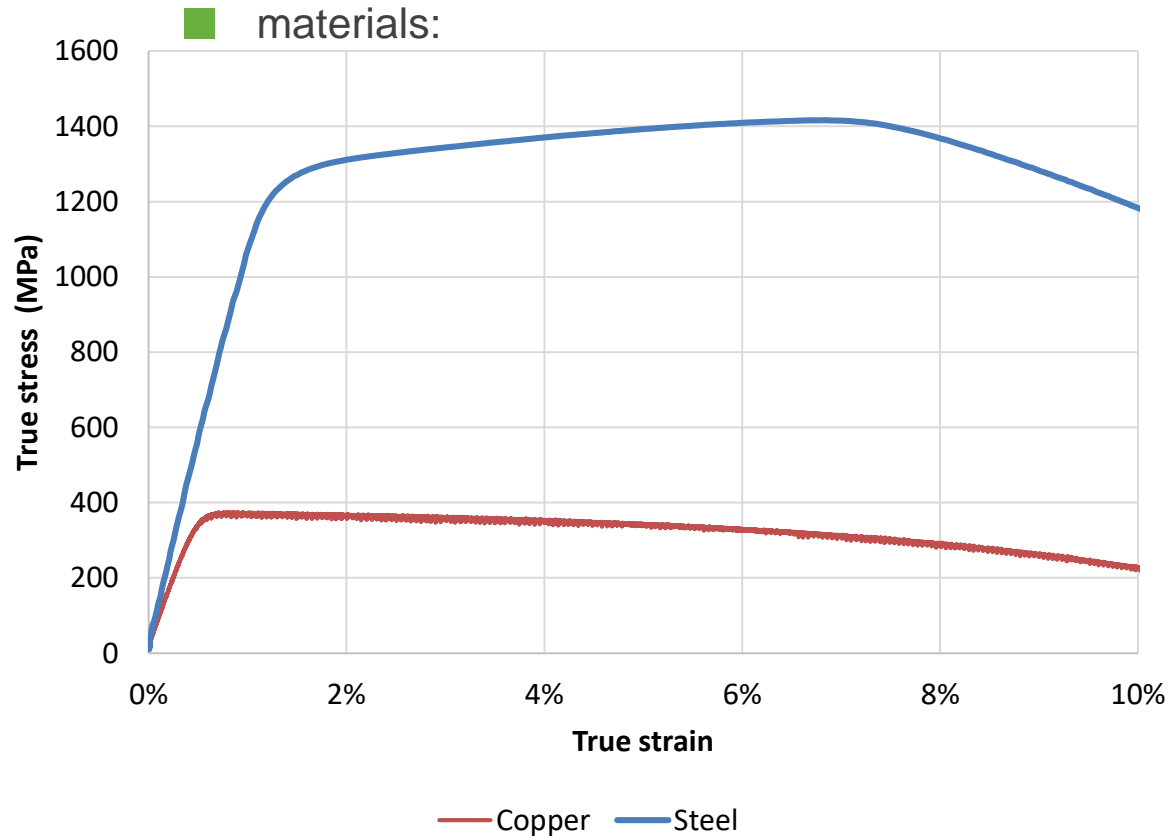


Fig. 9. Copper and steel stress-strain curves.

➔ The copper band will take most of the strain.

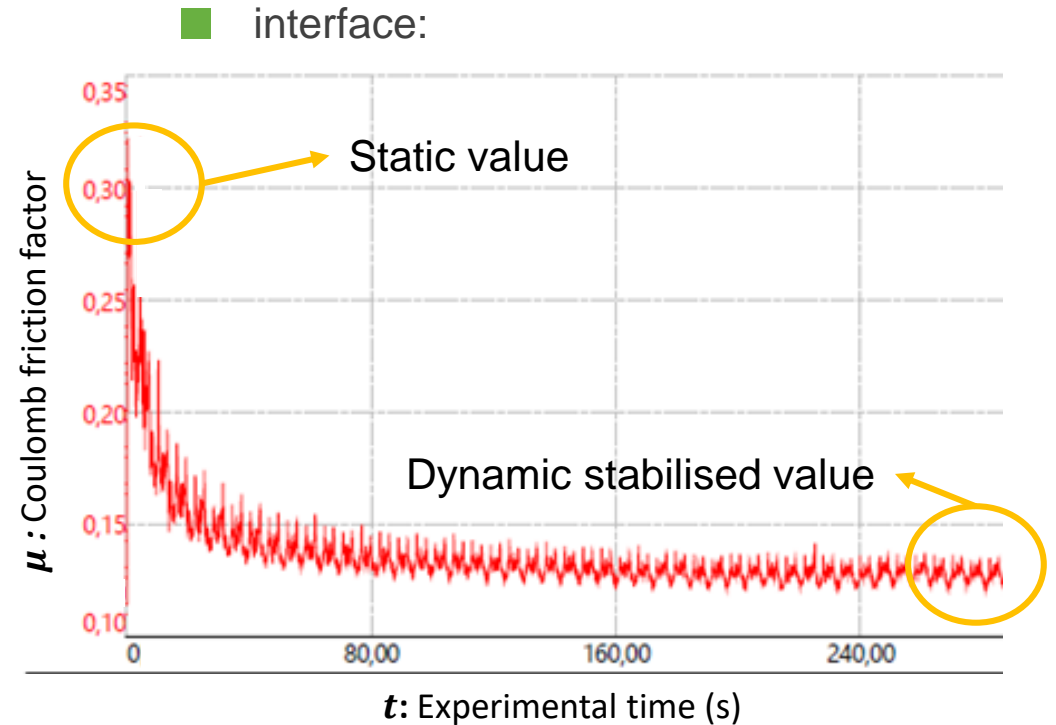


Fig. 10. Friction coefficient steel-copper on pin-disk tribometer.

➔  $\mu$  depends on materials and contact conditions.

➤ Characterisation campaign to obtain inputs for simulation.

- Energy loss is due to the implicit scheme instability for contact pairs: